

Computational Biophysics

RLE Group

Computational Biophysics Group

Academic and Research Staff

Professor Collin Stultz

Graduate Students

Elaine Gee,
Austin Huang,
Paul Nerenberg,
Christine Phillips,
Ramon Salsas-Escat,
Zeeshan Syed

Undergraduate Students

Veena Venkatachalam,
William Wyatt, Jr.

Collaborators

Prof. Catherine Drennan (MIT Chemistry)
Prof. John Gutttag (MIT, EECS)
Prof. D. E. Ingber (Harvard Medical School)

Technical and Support Staff

Arlene Wint

Introduction/Group Overview

The RLE Computational Biophysics Group is focused on understanding conformational changes in biomolecules that play an important role in common human diseases. The group uses an interdisciplinary approach combining computational modeling with biochemical experiments to make connections between conformational changes in macromolecules and disease progression. By employing two types of modeling, molecular dynamics and probabilistic modeling, hypotheses can be developed and then tested experimentally.

1. The Structure of Collagen and Collagenolysis

Sponsors:

National Science Foundation award no. MCB -- 0745638, Burroughs Wellcome Fund Contract no.1004339.01, W.M. Keck Foundation

Project Staff:

Paul Nerenberg, Prof. Collin Stultz

1.1 The Mechanism of Collagenolysis: A Substrate-centric View

Collagenolysis (collagen degradation) is a critical process in the progression of cancer metastasis, atherosclerosis, and other diseases. Despite considerable efforts to understand the steps involved, the exact mechanism of collagenolysis remains unknown. One proposed mechanism for collagenolysis suggests that the enzymes that degrade collagen, collagenases, physically unwind the triple-helical structure of collagen to gain access to the peptide bond that is cleaved. This unwinding mechanism would have large energetic requirements, but neither ATP nor other energy-rich molecules are necessary for collagenolysis. An alternative mechanism is that collagen exists in multiple states, some featuring structures that are unwound in the vicinity of the collagenase cleavage site, and that collagenases preferentially bind to and stabilize the unwound structures before degradation occurs.

The focus of this work is to investigate several aspects of this alternative mechanism using both experimental and computational methods. In particular, we used molecular dynamics simulations to explore the structure of human type I collagen in the vicinity of the collagenase cleavage site. Since post-translational proline hydroxylation is an important step in the synthesis of collagen chains, we used the DNA sequence for the $\alpha 1$ and $\alpha 2$ chains of human type I collagen with the known amino acid sequences for bovine and chicken type I collagen, to determine which prolines are hydroxylated in the vicinity of the collagenase cleavage site.

Simulations of type I collagen in this region suggest that partial unfolding of the $\alpha 2$ chain is energetically preferred relative to unfolding of the $\alpha 1$ chains. Localized unfolding of the $\alpha 2$ chain leads to a metastable structure that has disrupted hydrogen bonds N-terminal to the collagenase cleavage site. Our data suggest that this disruption in hydrogen bonding pattern leads to increased chain flexibility, thereby enabling the $\alpha 2$ chain to sample different partially unfolded states. Surprisingly, our data also imply that $\alpha 2$ chain unfolding is mediated by the non-hydroxylation of a proline residue that is N-terminal to the cleavage site in $\alpha 1$ chains. These results therefore suggest that hydroxylation on one chain ($\alpha 1$) can affect the structure of another chain ($\alpha 2$), and point to a critical role for the non-hydroxylation of proline residues near the collagenase cleavage site.

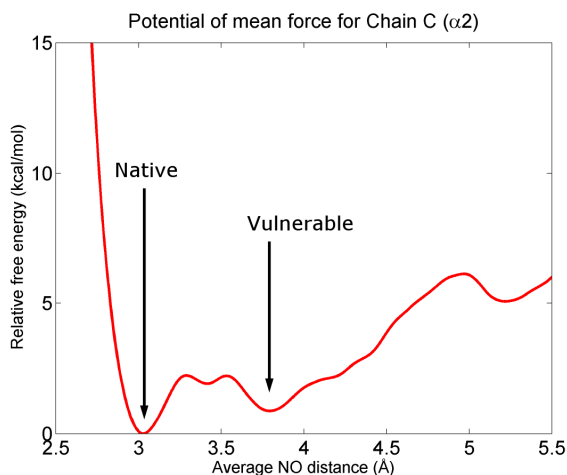


Figure 1: Potential of mean force for chain C ($\alpha 2$) of type I collagen showing both native and vulnerable states.

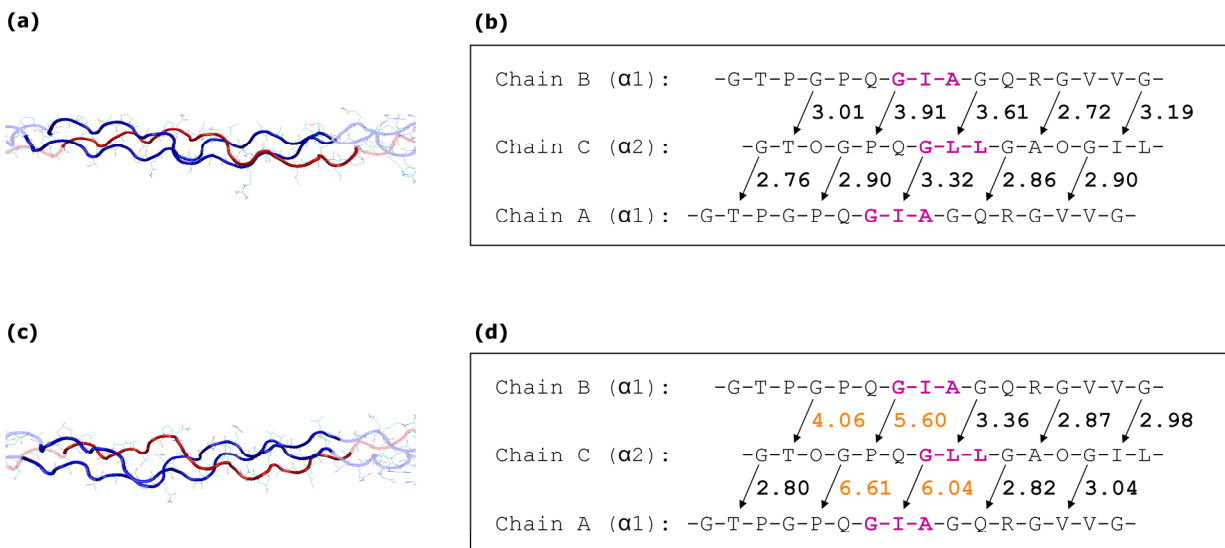


Figure 2: (a) Representative structure from the native state of type I collagen. The $\alpha 2$ chain is colored in red. (b) Interchain NO distances of the native state of type I collagen. The triplets containing the scissile bonds are colored in magenta. (c) Representative structure of the vulnerable state of type I collagen. (d) Interchain NO distances of the vulnerable state of type I collagen. NO distances greater than 4 Å are highlighted in orange.

2. The Role of Unfolded States in Collagen Degradation

Sponsors:

HST, RLE, Burroughs Wellcome Fund Contract no. 1004339.01, W.M. Keck Foundation

Project Staff:

Ramon Salsas-Escat, Prof. Collin Stultz

2.1 The Role of Unfolded States in Collagen Degradation

The hypothesis of this work is that collagen can undergo local unfolding near the cleavage site and that collagen degradation is the result of the interaction of **preformed** locally unfolded states in collagen and MMPs.

Using molecular dynamics as a tool, the particular structural features around the actual cleavage site of type III collagen were studied. It was shown that, out of the 5 potential cleavage sites in type III collagen, the actual cleavage site is the most vulnerable, locally unfolded and flexible of all. Moreover, under the hypothesis of locally unfolded states, the structural basis of a series of existing sequence rules that a cleavage site a series needs to accomplish in order to be degraded were established.

In order to obtain a model of collagen bound to MMP, both catalytic domain and full enzyme. Crystallography was initially chosen as the technique of use. The inactive catalytic domain of MMP8 (ICAT) was engineered out of the MMP8 sequence, purified and crystallized. A structure of the ICAT was obtained to a resolution of 1.75Å.

A rigid body docking methodology was developed in order to dock the lowest energy structures of collagen obtained in AIM1 into the ICAT structure. The best dock, corresponding to the actual cleavage site of type III collagen, can be then refined and molecular dynamics can be used in order to generate contact maps. Such contact maps constitute a dynamical model of collagen-MMP binding that can be tested in AIM3.

In order to initially validate the docking model of ICAT and type III collagen, degradation experiments involving the catalytic domain of MMP8 and type III collagen were carried out. The results showed unequivocally, and for the first time, that type III collagen can be degraded by the catalytic domain of MMP8 in the absence of the binding domain (Figure 1). These results support the use of the docking model as a starting structure to generate contact maps. Finally, mutants of MMP8 that eliminate the most important contacts with collagen will be tested for binding and degradation in order to validate the developed model.

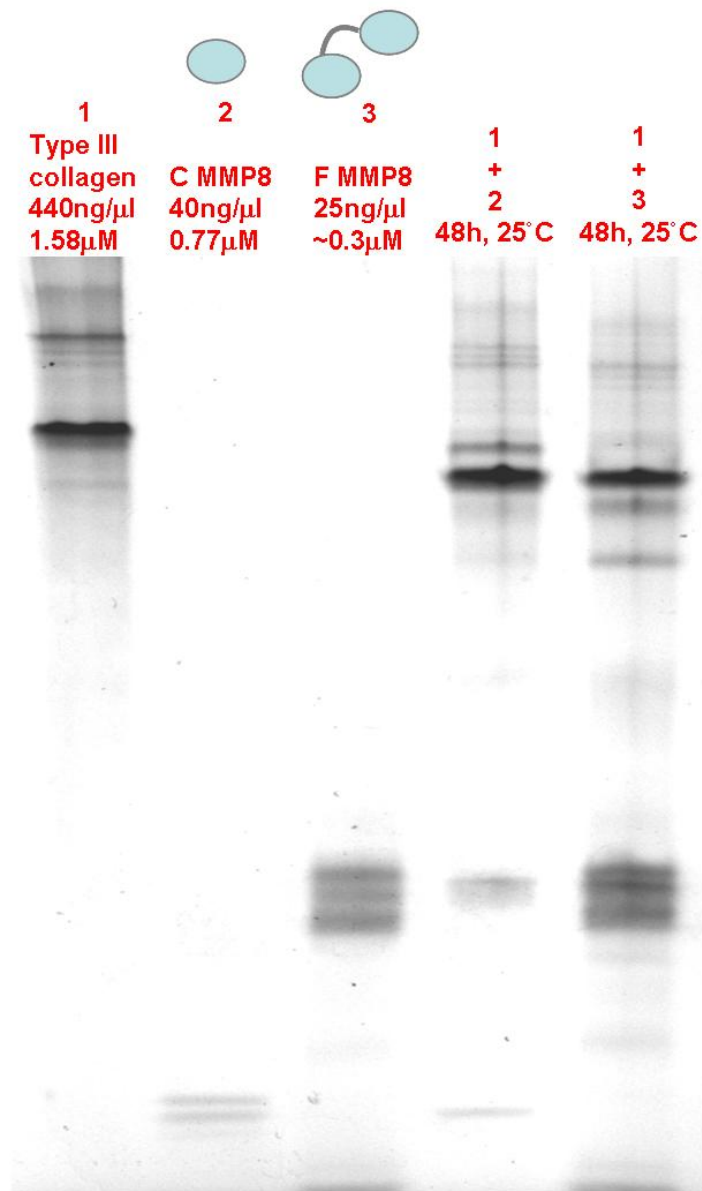


Figure 1. Degradation of type III collagen by different types of MMP8. Lane 1 is the type III collagen reference. Lanes 2 and 3 are the catalytic and full MMP8 references, respectively. Lane 4 shows the degradation of type III collagen by catalytic MMP8. Lane 5 shows the degradation of type III collagen by full length MMP8. The main degradation product in lanes 4 and 5, right below the band of collagen, shows that cleavage happens at the same location in both reaction.

3. Modeling the Unfolded State of Tau Protein

Sponsors:

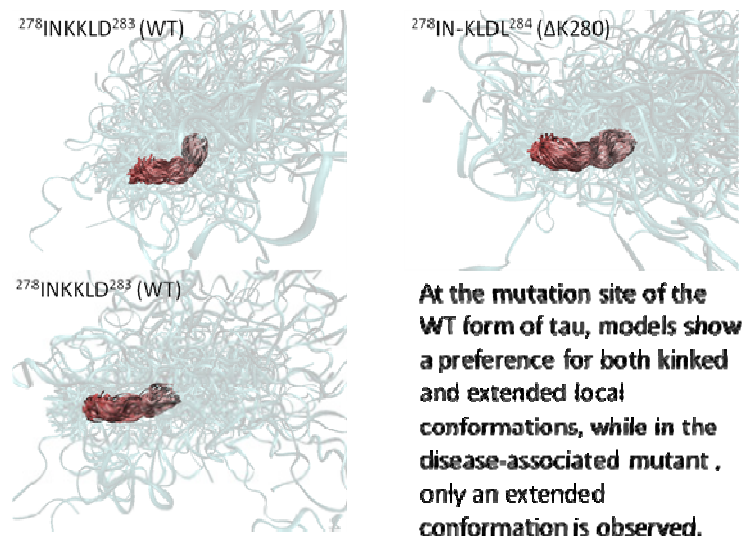
HST, RLE, Jonathan Allen Junior Faculty Award

Project Staff:

Austin Huang, Prof. Collin Stultz

3.1 The Effect of a Δ K280 Mutation on the Unfolded State of a Microtubule-Binding Repeat in Tau

Tau is a natively unfolded protein that forms intracellular aggregates in the brains of patients with Alzheimer's disease. To decipher the mechanism underlying the formation of tau aggregates, we developed a novel approach for constructing models of natively unfolded proteins. The method, Energy-minima Mapping and Weighting (EMW), samples local energy minima of subsequences within a natively unfolded protein and then constructs ensembles from these energetically favorable conformations that are consistent with a given set of experimental data. Using EMW we generated ensembles that are consistent with chemical shift measurements obtained on ^{13}C enriched tau constructs. Thirty models were constructed for the second microtubule binding repeat (MTBR2) in wild-type (WT) tau and a Δ K280 mutant, which is found in some forms of frontotemporal dementia. We find that the aggregation-initiating sequence, PHF6*, prefers an extended conformation in both the WT and Δ K280 sequences. In addition, we find that residue K280 can adopt a loop/turn conformation in solution and that deletion of residue, which can adopt non-extended states, results in an increase in locally extended conformations in the vicinity of PHF6*. As an increased preference for extended states downstream from PHF6* likely facilitates downstream propagation of β -structure in Δ K280 mutants, these results explain how a deletion at position 280 can promote the formation of tau aggregates.



4. Intrinsically Unstructured Proteins

Sponsors:

HST, RLE, Burroughs Wellcome Fund Contract no. 1004339.01

Project Staff:

Veena Venkatachalam, Austin Huang, Prof. Collin Stultz

4.1 Intrinsically Unstructured Proteins

Intrinsically unstructured proteins (IUPs) play essential roles in protein-protein signaling, but unlike globular proteins, they can adopt a variety of distinct conformations in solution. This conformational flexibility is thought to facilitate their ability to bind multiple substrates. We study the p21 protein, a small IUP (164 residues) that binds to approximately 25 targets and is ubiquitous in cellular signaling, e.g., cell cycle control, apoptosis, transcription, differentiation, etc. Our studies focus on understanding the ability of this small, unstructured protein to recognize each of its targets with high affinity.

To understand the structural plasticity of p21, we study a 20-residue peptide derived from the C-terminus of p21 (p21¹⁴⁵⁻¹⁶⁴). The N-terminal half of this peptide, p21¹⁴⁷⁻¹⁵⁴, has a significant helical propensity which is recognized by some binding partners, while the C-terminus, p21¹⁵⁵⁻¹⁶⁰, prefers extended conformations that facilitate binding to proliferating cell nuclear antigen (PCNA). Using molecular dynamics simulations, we construct ensembles for p21¹⁴⁵⁻¹⁶⁴ that are consistent with NMR data and demonstrate that the peptide adopts a number of distinct structural states in solution, where some of these states are similar to experimentally observed bound conformations of the peptide. Our results suggest that the final bound conformations of p21¹⁴⁵⁻¹⁶⁴ pre-exist in the free peptide. While the conformational flexibility of the p21 peptide is essential for adapting to diverse binding environments, the peptide's intrinsic structural preferences enable promiscuous - yet high affinity - binding to a diverse array of molecular targets.

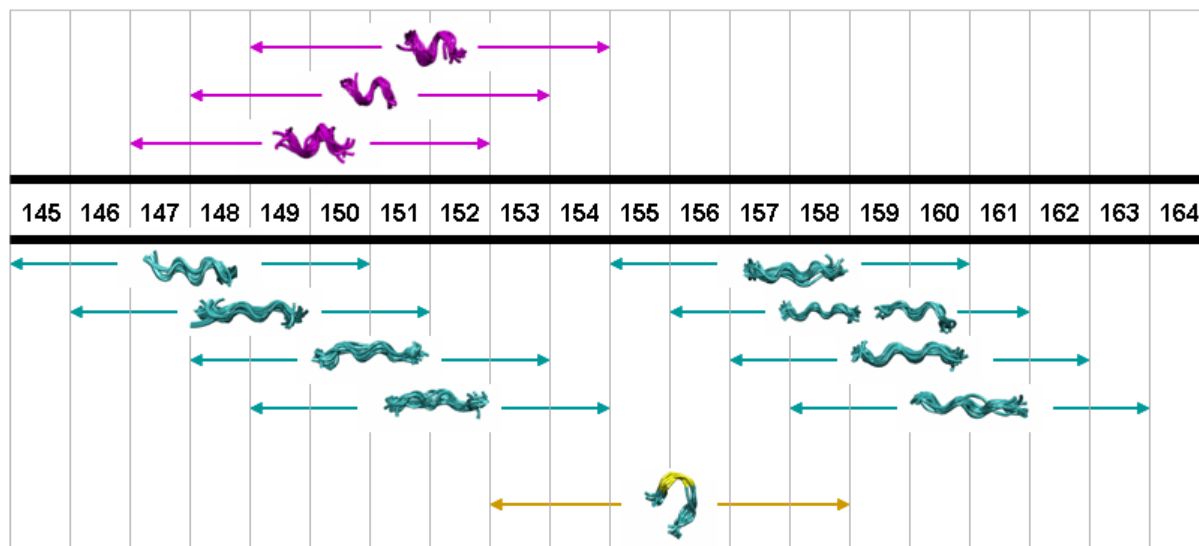


Figure 3. Linear representation of the p21 peptide studied showing conserved 6-residue structural motifs. Helical conformations are colored purple and extended regions are shown in cyan. The region corresponding to a turn is colored yellow.

5. Computational Studies of Nickel Regulatory Protein NikR

Sponsors:

HST, RLE, Jonathan Allen Junior Faculty Award, Drennan's Project Sponsor No.???

Project Staff:

Prof. Catherine Drennan, Christine Phillips, Prof. Collin Stultz

5.1 NikR: A Brief Introduction to the Problem

Regulation of transition metals in the cell is crucial for all living organisms. While some enzymes require metals to function properly, an excess of metal ions in the cell can induce apoptosis. Over recent years, the nickel regulatory system has gained interest due to its crucial role in *H. pylori* infection and a number of researchers now study this pathway. The key regulator in the pathway, NikR, has been extensively, with publications documenting binding of different transition metals (1, 2), DNA binding affinities (1, 3, 4), structural attributes (5-7), and stabilization requirements (2, 8, 9), to name a few. Mainly these studies have been completed with the *E. coli* homolog (EcNikR). While these studies have begun to elucidate the mechanism of NikR, they have also raised a number of questions that need to be answered to fully understand the NikR system.

A previous *in vitro* study has shown that EcNikR binds DNA more tightly in the presence of excess nickel ions in comparison to the form with stoichiometric nickel ions (K_d of 2×10^{-11} M) compared to stoichiometric nickel ions (K_d of 5×10^{-9} M) (1). Our computational studies aims to determine whether there is a single nickel site or a series of sites that account for the increased affinity and to examine the possible location(s) of these sites. Currently, there are two proposed possibilities for the location(s) of these sites. The first possibility is at the interface of the central portion of the structure and the DNA binding portion (shown in Fig. 1 in pink spheres). However, when a structure of EcNikR-DNA was published it indicated potassium, not nickel, binding in this site.

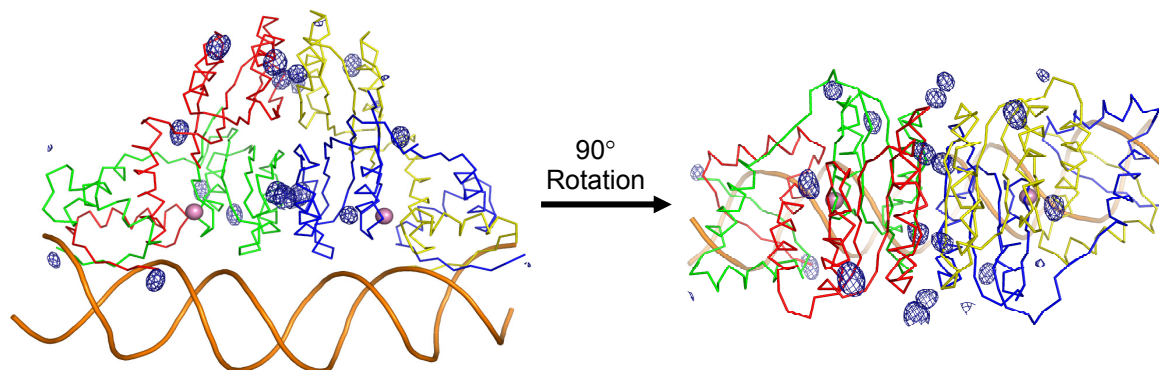


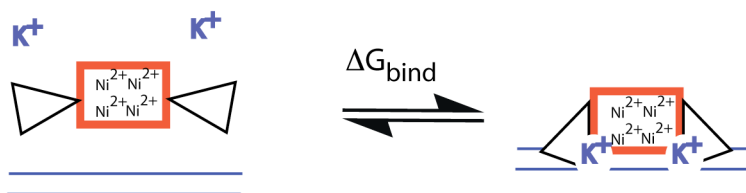
Figure 1. Metal binding sites on NikR. Protein is represented in ribbons in red, green, blue, and yellow with DNA in orange. Extra nickel binding sites on the surface of NikR with nickel ions represented in blue mesh. Potassium ions are shown in pink (7).

Crystallographic studies of EcNikR bound to DNA with excess nickel present indicated that excess nickel ions did not bind in a single specific site, but bound to unconserved histidines on the surface of the protein (Fig. 1) (7). The second proposal for the location of these excess nickel binding sites is at these locations on the surface of the protein (shown in Fig. 1 in mesh). Using Poisson-Boltzmann directed

electrostatic computations we hope to: (1) illustrate that the first site proposed for excess nickel binding is actually a potassium site and (2) probe the sites seen in the excess nickel-soaked structure to determine which, if any, of these sites is responsible for the increased NikR-DNA affinity.

5.2 Simplifying the Computational Problem

The overall DNA binding reaction can be expressed as:



The overall binding energy can be decomposed into two terms:

$$(1.1) \quad \Delta G_{bind} = \Delta G_{elec} + \Delta G_{non-elec}$$

We will assume that the differences in binding arise primarily from the electrostatic term. Use of this approximation in highly charged systems is supported by prior studies which demonstrate that fruitful results can be obtained by computing the electrostatic contribution alone (10, 11). Hence, questions of relative binding affinity may be adequately addressed by focusing on the electrostatic contribution.

We will use the Poisson-Boltzmann method to determine how different residues in the protein affect the relative affinity of EcNikR for DNA.

Central to the Poisson Boltzmann (PB) formalism is the assumption that the protein can be modeled as a collection of charges embedded in a low dielectric medium. The overall electrostatic free energy is given by the linearized PB equation:

$$(1.2) \quad \nabla \cdot [\epsilon(r) \nabla \phi(r)] - \kappa^2 \phi(r) = -4\pi\rho(r)$$

where $\phi(r)$ is the electrostatic potential energy, $\epsilon(r)$ is the position dependent dielectric constant, $\rho(r)$ is the charge density, and κ^2 is the Debye-Huckel screening constant (which is related to ionic strength).

The electrostatic free energy of a given protein binding event, ΔG_{elec} , with a fixed conformation can be written as the sum of the solvation energy plus a Coulombic energy term:

$$(1.3) \quad \Delta G_{elec} = \Delta G_{solv} + C$$

where C is the Coulombic interaction energy in vacuum. The key point here is that the solvation energy can be expressed as the difference of two electrostatic free energies:

$$(1.4) \quad \Delta G_{solv} = \Delta E_{wat} - \Delta E_{vac}$$

Once the electrostatic potential, $\phi(r)$, is known, the total electrostatic free energy (relative to a reference state where all charges are infinitely separated) is given by:

$$(1.5) \quad \Delta E_{wat} = \sum_i \left(\frac{q_i \phi_i(r_i)}{2} \right)_{\epsilon_{ext}=80}$$

Using this formalism, it is easy to show that:

$$(1.6) \quad \Delta G_{elec} = \sum_k \Delta G_{a_k}$$

where ΔG_{a_k} is the contribution of the k^{th} residue, a_k to the overall electrostatic free energy. Here we note that the term residue can refer to an amino-acid in the protein or a bound ion.

Equation 1.6 demonstrates that we can calculate the contribution of every residue to the overall electrostatic free energy. This allows us to identify residues (or ions) that make significant contributions to the protein's affinity to DNA.

To ensure that the calculated ΔG is robust, we will use molecular dynamics to generate an ensemble of ten starting structures of NikR and will repeat the PB calculation on each of these structures to determine if the change in free energy for each is comparable.

5.3 Applying Computational Methods to The Excess Nickel Question

With these calculations, we would like to investigate whether potassium or nickel is preferred at the site located between the central and DNA binding domains. Computationally, we will specifically determine the difference in free energy change upon binding with potassium or nickel bound in this site (Fig. 2).

One way to calculate this difference is to determine the change in free energy upon binding DNA with nickel (Fig. 2, I \rightarrow III, ΔG_2) and similarly with potassium (Fig. 2, I \rightarrow II, ΔG_1). Subtracting these changes in free energy we can determine the effect excess nickel has on DNA binding affinity ($\Delta\Delta G = \Delta G_1 - \Delta G_2$). We can simplify this calculation using the PB formalism and simply calculate the difference in free energy between the potassium and nickel bound states directly (Fig.2, II \rightarrow III, ΔG_3).

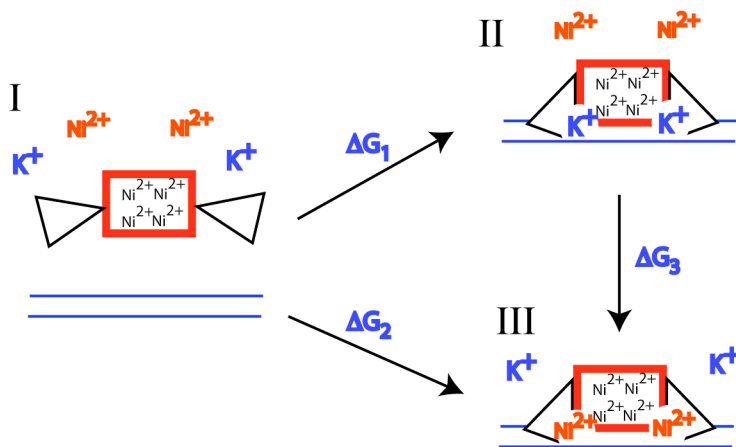


Figure 2. Thermodynamic box illustrating our technique for computational analysis of the effect of the excess nickel binding sites.

From the PB calculations we can also determine the impact each amino acid has on the overall free energy difference of the structures and therefore which amino acids may be crucial for explaining the preference for potassium over nickel. Following these initial calculations, a similar approach will be taken to examine the nickel binding sites on the exterior of the protein.

References

- 1 Bloom, S. L., and Zamble, D. B. (2004) Metal-Selective DNA-Binding Response of *Escherichia coli* NikR, *Biochemistry* 43, 10029-10038.
- 2 Wang, S. C., Dias, A. V., Bloom, S. L., and Zamble, D. B. (2004) Selectivity of Metal Binding and Metal-Induced Stability of *Escherichia coli* NikR, *Biochemistry* 43, 10018-10028.
- 3 Chivers, P. T., and Sauer, R. T. (2002) NikR Repressor: High-Affinity Nickel Binding to the C-Terminal Domain Regulates Binding to Operator DNA, *Chem. Biol.* 9, 1141-1148.
- 4 Abraham, L. O., Li, Y., and Zamble, D. B. (2006) The metal- and DNA-binding activities of *Helicobacter pylori* NikR, *J. Inorg. Biochem.* 100, 1005-1014.
- 5 Dian, C., Schauer, K., Kapp, U., McSweeney, S. M., Labigne, A., and Terradot, L. (2006) Structural Basis of the Nickel Response in *Helicobacter pylori*: Crystal Structures of HpNikR in Apo and Nickel-bound States, *J. Mol. Bio.* 361, 715-730.

- 6 Schreiter, E. R., Sintchak, M. D., Guo, Y., Chivers, P. T., Sauer, R. T., and Drennan, C. L. (2003) Crystal structure of nickel-responsive transcription factor NikR, *Nat. Struct. Bio.* 10, 794-799.
- 7 Schreiter, E. R., Wang, S. C., Zamble, D. B., and Drennan, C. L. (2006) NikR-operator complex structure and the mechanism of repressor activation by metal ions, *Proc. Natl. Acad. Sci. U. S. A.* 103, 13676-13681.
- 8 Dias, A. V., and Zamble, D. B. (2005) Protease digestion analysis of *Escherichia coli* NikR: evidence for conformational stabilization with Ni(II), *J. Bio. Inorg. Chem.* 10, 605-612.
- 9 Leitch, S., Bradley, M. J., Rowe, J. L., Chivers, P. T., and Maroney, M. J. (2007) Nickel-Specific Response in the Transcriptional Regulator, *Escherichia coli* NikR, *J. Am. Chem. Soc.* 129, 5085-5095.
- 10 Honig, B., and Nicholls, A. (1995) Classical Electrostatics in Biology and Chemistry, *Science* 268, 1144-1149.
- 11 Norberg, J. (2003) *Archives of Biochemistry and Biophysics* 410, 48-68.

6. Modeling Physiologic Unfolding of Fibronectin with Steered Molecular Dynamics Simulation

Sponsors:

HST, RLE, Burroughs Wellcome Fund Contract no. 1004339.01

Project Staff:

Elaine Gee, Prof. D.E. Ingber, Prof. Collin Stultz

6.1 Cell-Mediated Fibronectin Unfolding

When a particular Fibronectin (FN) polymerization is essential for the development and repair of the extracellular matrix, but the molecular details of FN fibril formation are unclear. Data suggest that FN fibrillogenesis is facilitated by cell traction forces transferred to FN via bound membrane integrin receptors. Forces applied to distinct regions of FN drive the formation of partially unfolded FN intermediates that then bind to additional FN molecules. Past studies have focused on FN unfolding by pulling at the N- and C-termini rather than at the site of cell binding. However, since cell membrane integrins bind FN at a surface-exposed RGD loop in the 10th repeat of its type III FN domains (10FNIII), we investigate the mechanism of cell-mediated FN unfolding by using steered molecular dynamics to apply tensile force at the RGD site. While pulling at the N- and C-termini leads to unfolding trajectories that sample different unfolding pathways as previously published, we find that pulling at the RGD site unfolds 10FNIII along one well-defined pathway. This pathway accesses a partially unfolded intermediate structure with solvent exposed hydrophobic N-terminal residues. Moreover, additional unfolding of this intermediate triggers an arginine residue, which is required for high affinity cell binding, to separate from the adjacent RGD loop. Based on these results, we propose a mechanism by which cell traction induces a conformation change in FN that not only drives FN fibril formation but also allows for cell detachment, thereby promoting the binding of new FN to the cell surface receptor to promote subsequent cycles of adhesion, unfolding, and fibril formation that drive FN matrix assembly (Figure 1). Currently, investigations are underway to provide experimental support for the proposed mechanism obtained from these computational simulations.

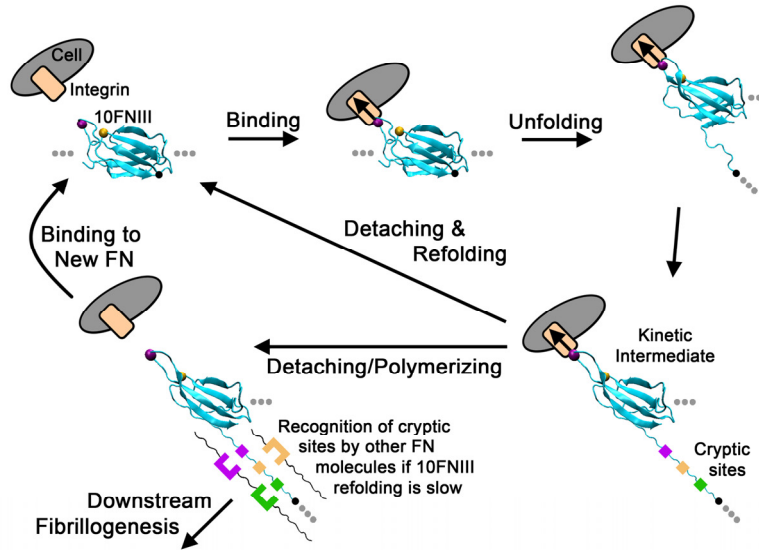


Figure 1. Cell-mediated Fibrillogenesis. The proposed model involves the formation of a partially unfolded intermediate during cell-traction mediated unfolding. Potential cryptic sites may exist in this partially unfolded structure that promote FN aggregation and fibrillogenesis.

Subsequent unfolding past this intermediate induces a crucial arginine (gold bead) at a secondary binding site to move to a position far from the RGD loop (central glycine labeled by magenta bead). This frees the cell and enables it to reattach to another FN molecule to propagate the process. If 10FNIII refolding is relatively slow, then unfolded portions of this domain can make contacts with other FN molecules to stimulate downstream fibrillogenesis.

7. ECG Markers to Predict Cardiovascular Death

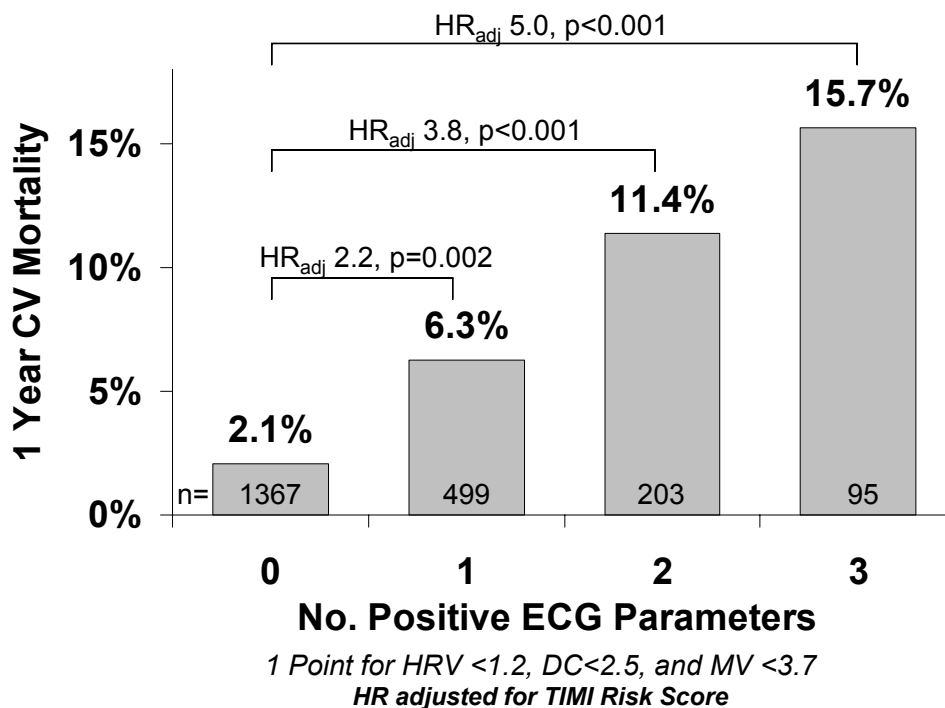
Sponsors:
HST, RLE

Project Staff:
Zeeshan Syed, Prof. Collin Stultz, Prof. John Guttag

ECG parameters such as heart rate variability (HRV), deceleration capacity (DC) and morphologic variability (MV) may help identify patients at high risk post-ACS. These techniques measure specific aspects of cardiac health. HRV studies sympathovagal modulation of heart rate, DC extends heart rate turbulence by measuring acceleration-deceleration patterns, and MV quantifies variability in the shape of the ECG signal associated with myocardial instability. We are assessing the relationship among HRV, DC and MV, and cardiovascular (CV) death after NSTEMI/ACS.

We have explored the effect of different ECG based risk scores on predicting patients who are at high risk of death following NSTEMI/ACS.

CV Death According to Number of Positive ECG Parameters



Publications

Journal Articles, Published

E.P.S. Gee, D.E. Ingber, and C.M. Stultz, "Fibronectin Unfolding Revisited: Modeling Cell traction-Mediated Unfolding of the Tenth Type-III Repeat," *PLoS ONE* 3(6): e2373. doi:10.1371/journal.pone.0002373 (2008).

R. Salsas-Escat, and C.M. Stultz, "The Molecular Mechanics of Collagen Degradation: Implications for Human Disease," *Experimental Mechanics* (Published online ahead of print DOI10.1007/s11340-007-9105-1) (2008).

P.S. Nerenberg, R. Salsas-Escat, C.M. Stultz, "Do Collagenases Unwind Triple-Helical Collagen Prior to Peptide Bond Hydrolysis? Reinterpreting Experimental Observations with Mathematical Models," *Proteins: Structure, Function, and Bioinformatics* 70: 1154-1161 (2008).

Z. Syed, J. Guttag, and C.M. Stultz, "Clustering and Symbolic Analysis of Cardiovascular Signals: Discovery and Visualization of Medically Relevant Patterns in Long-Term Data Using Limited Prior Knowledge," *EURASIP Journal on Advances in Signal Processing*, 2007: Article ID 67938, 16 pages (2007).

P.S. Nerenberg, R. Salsas-Escat, C.M. Stultz, "Collagen --- A Necessary Accomplice in the Metastatic Process," *Cancer Genomics and Proteomics* 4: 319-328 (2007).

A. Thomas, E.R. Edelman, C.M. Stultz, "Collagen Fragments Modulate Innate Immunity," *Exp. Biol. & Med.*, 232: 406-411 (2007).

A. Huang, and C.M. Stultz, "Conformational Sampling with Implicit Solvent Models: Application to the PHF6 Peptide in Tau Protein," *Biophys. J.* 92: 34-45 (2007).

Journal Articles, Accepted for Publication

A. Huang, and C.M. Stultz, "The Effect of a Δ K280 Mutation on the Unfolded State of a Microtubule-Binding Repeat in Tau," *PLoS Comp. Bio.*, forthcoming.

P.S. Nerenberg, and C.M. Stultz, "Differential Unfolding of α 1 and α 2 chains in Type I Collagen and Collagenolysis," *JMB* forthcoming

Journal Articles, Submitted

Z. Syed, C. Stultz, M. Kellis, P. Indyk and J. Gutttag, "Motif Discovery in Physiological Datasets: A Methodology for Inferring Predictive Elements."

Z. Syed, B.M. Scirica, S. Mohanavelu, C.P. Cannon, P.H. Stone, E.L. Michelson, C.M. Stultz and J.V. Gutttag, "Beyond Heart Rate Variability: Exploiting Variation in ECG Beat Morphology to Identify Patients at Risk of Death Following Non-ST-Elevation Acute Coronary Syndromes."

Z. Syed, B. Scirica, S. Mohanavelu, D. Morrow, C. Stultz and J. Gutttag, "ECG Markers to Predict Cardiovascular Death: Heart Rate Variability, Deceleration Capacity and Morphologic Variability in Non-ST-Elevation ACS from the MERLIN-TIMI 36 Trial."

Z. Syed, B. Scirica, D. Morrow, C. Stultz, and J. Gutttag, "Beyond Heart Rate Variability: Supplementing Variability in the Length of Heart Beats with Variability in Morphology."

Meeting Papers, Accepted for Publication

Z. Syed, B.M. Scirica, C.M. Stultz, and J.V. Gutttag, "Risk-Stratification Following Acute Coronary Syndromes Using a Novel Electrocardiographic Technique to Measure Variability in Morphology," *Computers in Cardiology* 2008.

Z. Syed, B.M. Scirica, C.M. Stultz, and J.V. Gutttag, "Comparing Symbolic Representations of Cardiac Activity to Identify Patient Populations with Similar Risk Profiles," *Computers in Cardiology* 2008.

